

Determination of the Deep Optical Properties of Healthy and Diseased Skin Using Diffuse Reflectance Spectroscopy

Didier K. Yable^{1,2} , Laurent Canale^{1*} , Théodore Cissé Haba² , Pascal Dupuis¹ ,
Georges Zissis¹ , Zoueu T. Jérémie² 

¹LAPLACE, Université de Toulouse, CNRS, INPT, UPS, Toulouse, France

²L2IS, École Doctorale Polytechnique, UMRI 78, INP-HB, Yamoussoukro, Côte d'Ivoire

Email: *laurent.canale@laplace.univ-tlse.fr

How to cite this paper: Yable, D.K., Canale, L., Haba, T.C., Dupuis, P., Zissis, G. and Jérémie, Z.T. (2022) Determination of the Deep Optical Properties of Healthy and Diseased Skin Using Diffuse Reflectance Spectroscopy. *Optics and Photonics Journal*, 12, 191-199.

<https://doi.org/10.4236/opj.2022.128014>

Received: May 27, 2022

Accepted: August 19, 2022

Published: August 22, 2022

Copyright © 2022 by author(s) and Scientific Research Publishing Inc.

This work is licensed under the Creative Commons Attribution International License (CC BY 4.0).

<http://creativecommons.org/licenses/by/4.0/>



Open Access

Abstract

In this study, we focused on diffuse reflectance spectroscopy, a rapid and noninvasive spectroscopy technique that has considerable potential for medical diagnosis. In order to better understand and analyze the signals induced by this method, we performed a series of *in vivo* measurements on healthy and diseased skin. Measurement sites on a human hand and feet were chosen. Some preliminary results obtained on these sites show the feasibility of this technique in clinics.

Keywords

Diffuse Reflectance Spectroscopy, Human Skin, Optical Properties, Lesion, Signal

1. Introduction

Diffuse reflectance spectroscopy (DRS) is a rapid and non-invasive technique that has considerable potential in many biomedical applications.

Compared to autofluorescence, this method by diffuse reflectance implies a strong intensity of the diffusion signal and thus makes it possible to have a better signal/noise ratio. This method is less traumatic for the patient and does not require a biopsy. Furthermore, this system is inexpensive, simple to implement and rapid and could also be applied to diagnoses of cancer of the skin, on the tissues of the colon, the bladder, the breast, or the mouth. This technique is therefore very promising for *in vivo* diagnosis in oncology.

Biomedical applications are such as burn depth assessment, [1] [2] [3] cancer diagnosis and treatment [4] [5] monitoring of tissue oxygenation, classification

of healthy and pathological dental tissue [6] [7], blood glucose monitoring [8] [9] [10] [11]. By injecting light onto a tissue, DRS determines the optical properties of biological tissues [12] and detects the reflected intensity after successive scattering and absorption events [13]. This technique also allows the quantification of differentiation between normal and diseased tissues [14]. Most of the time, DRS spectra can be acquired in two ways, namely by point spectroscopy or by hyper spectral imaging [15] [16]. Thus DRS constitutes an important tool for the differentiation and classification of pathological tissues. On the other hand, knowledge of the optical properties of the skin is a key issue in the management of patients with a large number of pathological tissues. In this context, we used a low-cost optical instrument based on spatially resolved diffuse reflectance spectroscopy [17]. Our goal here is to quantify the reflection coefficient of healthy and diseased skin. Human skin has been studied by diffuse reflectance spectroscopy in the spectral range of 380 nm to 780 nm. First, we presented the system and the methodology used. Next, we present the results of the measurements and show how we adapted the processing method to analyze the different parts of the skin. Finally, on the skin *in vivo*, the measurements that were carried out with this methodology on the healthy skin of volunteers and near the Buruli ulcer are presented.

2. Materials and Methods

2.1. Experimental Configuration

The measurement system we use in this study is shown in **Figure 1**. It consists of a Spectroradiometer Specbos 1201 (**Figure 1(a)**), which uses two broadband photo lamps as an illumination source (**Figure 1(d)**). Additionally, a Labsphere (**Figure 1(b)**) featuring a diffusely reflective white coating was used in the UV-VIS-NIR spectral range. Additionally, a Labsphere 1(b) figure, featuring a diffusely reflective white coating, was used in the UV-VIS-NIR spectral range. A computer (**Figure 1(c)**) allows precise control of the acquisition measurement in less than one hundred and eighty seconds and processes the acquired data in order to extract the reflectance properties.

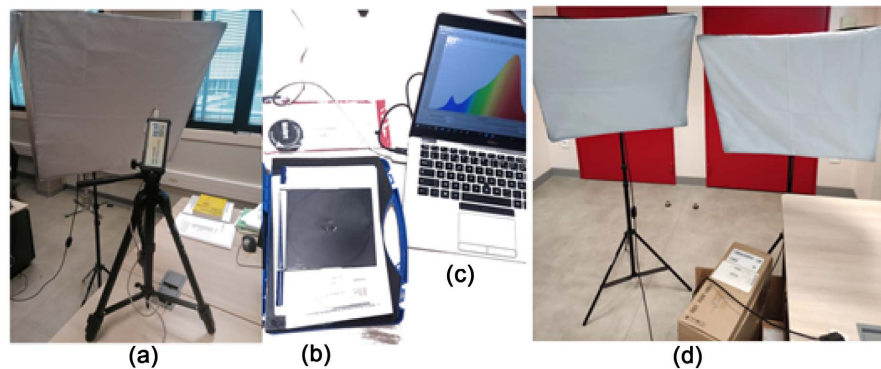


Figure 1. Overview of the measurement system used: (a): Spectroradiometer specbos 1201; (b): Labsphere; (c): computer; (d): Photos lamps.

2.2. Samples

We performed the measurements on the skin surface of four human volunteers (with different skin colors, male) without any specific criteria or preprocessing. Two measurement sites were selected. We have respectively, the skin in the middle of the wrist fold (site I), finally the back of the hand (site II) (**Figure 2**). Additionally, the tissues from the two selected measurement sites should provide appropriate information about the unique tissue-related properties of the induced spectral response.

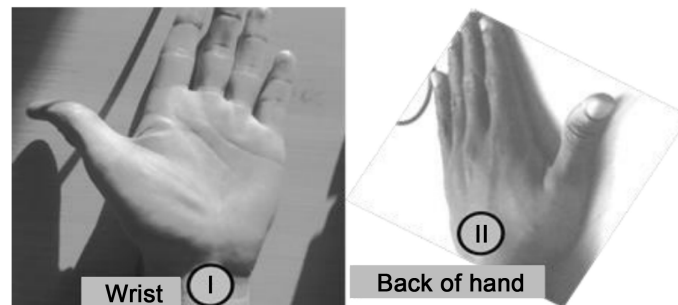


Figure 2. Illustration of the two selected measurement sites: Skin above the wrist crease (site I) and the skin on the back of hand (site II).

3. Measurements and Analysis

The measurements presented here are measurements carried out on healthy skin. They were performed with the experimental setup shown in **Figure 1**. We first selected the two skin sites described above and measurements were taken for each. During the data acquisition process (beginning with a linear activation of the “target” which stops after 120 to 180 seconds), the hands of the volunteers were held down in order to avoid any measurement errors. Spectral data were acquired synchronously. A total of 29 spectra were acquired. This range was chosen based on the operation of our device. Nine measurements were taken for each of the two selected skin sites, I: skin above the wrist crease, and II: skin on the dorsum of the hand). About 4 to 5 minutes were needed to edit and export the measurement. In this way, we obtained 18 measurements for each of the volunteers. We evaluated the reflectance factor and processed the acquired data.

3.1. Reflectance Factor Calculation and Spectra Processing

The spectral reflectance factor of a given skin tissue sample at each wavelength can be calculated from the following equation:

$$R(\lambda) = \frac{S(\lambda) - S_d(\lambda)}{S_s(\lambda) - S_d(\lambda)} \times R_s \quad (1)$$

where S is the signal intensity of a wavelength scan of a skin sample λ , S_s is the reference signal of standard λ , S_d is the spectrum of the length λ , and R_s is the percent spectral reflectance of the substituted λ standard from Equation (1).

Next, the spectra were processed according to the calibration methodology based on the reflectance spectrum S_r .

3.2. Acquisition and First Observations

We acquired data on these two samples as described above, and the optical coefficient spectra of the samples are extracted from these acquisitions as presented above. The difference in scattering levels between the different sites is clearly visible in **Figure 3** and **Figure 4**. On the reflectance spectrum extracted from site I, only in **Figure 3**, an evolutionary difference is detected.

3.3. Results

We present the results of the measurements performed on the two selected skin sites. The spectrum showed significant changes. In this way, we evaluated sites II and III. The reflectance spectra observed by the simulation are shown in **Figure 4**. The average reflectance changes regularly at the two measurement sites. Various significant peaks are observed, the reflectance values of which are recorded

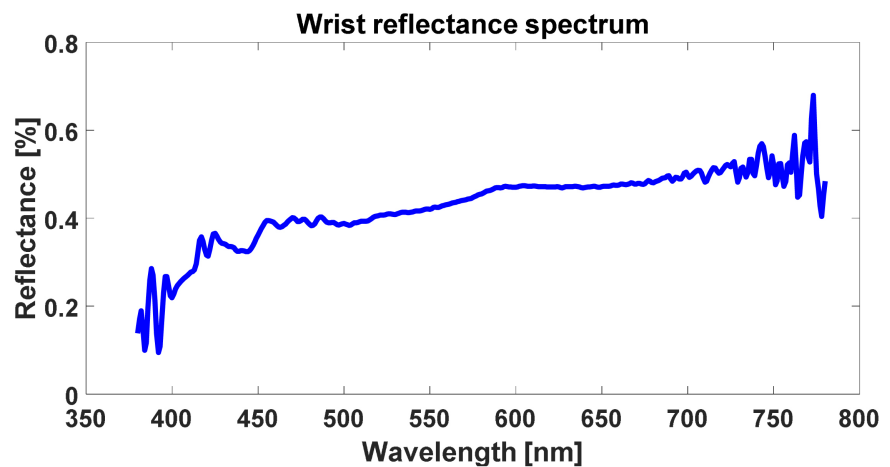


Figure 3. Reflectance profile of the wrist of the hand as function of wavelength.

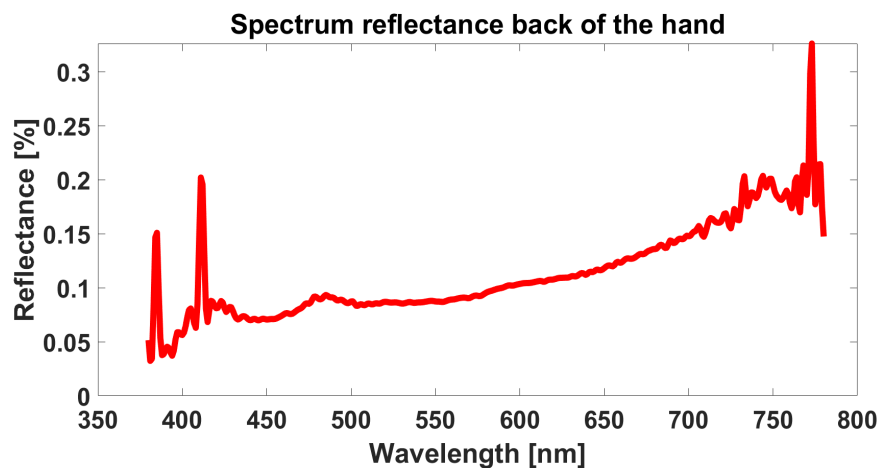


Figure 4. Spectral profile of the back of the hand as a function of wavelength.

in **Table 1** and **Table 2**. These peaks are potentially due to the echoes of the chromophores.

Figure 4 shows the performance of our measurement evaluation over the entire range. It can be seen that the reflectance spectra of the two sites show essentially the same patterns with significant peaks.

On this spectral region from 380 to 780 nm, we have three significant peaks acquired respectively at wavelengths 385 nm, 420 nm then the last peak at 773 nm with the site I. It is clear that the reflectance value depends on the measurement site. We found that in the spectral region of 350 to 450 nm, the wrist of the hand shows higher reflectance values than the back of the hand with a button. He noted that the wrist of the hand is more sensitive than the back of the hand, so the reflectance depends on the measurement site.

The spectral changes and their impact on the two measurement sites were studied in the spectral range of 380 to 780 nm. With respect to the optical window, i.e., the spectral from 380 to 780 nm, the reflectance of the sites is clear. The observed spectral changes are consistent with the sites. The more sensitive the site, the higher the reflectance values and the more diffusive the site. However, a better quantification is obtained for site I than for site II and a weaker influence of site I, as shown in **Figure 5**. Therefore, the evaluation of site properties is less sensitive to the absorption of the upper site. Thus, by applying this method to the characterization of the skin, the dermis can be scanned under the influence of the melanin contained in the epidermis.

Table 1. Wrist reflectance value a function of wavelength.

Wavelength [nm]	Reflectance [%]
382	0.19
388	0.29
396	0.27
455	0.40
744	0.56
773	0.68

Table 2. Reflectance value of the wrist to be erased the back of the hand.

Wavelength [nm]	Reflectance [%]
382	0.19
385	0.15
388	0.29
396	0.28
411	0.20
744	0.57
773	0.68

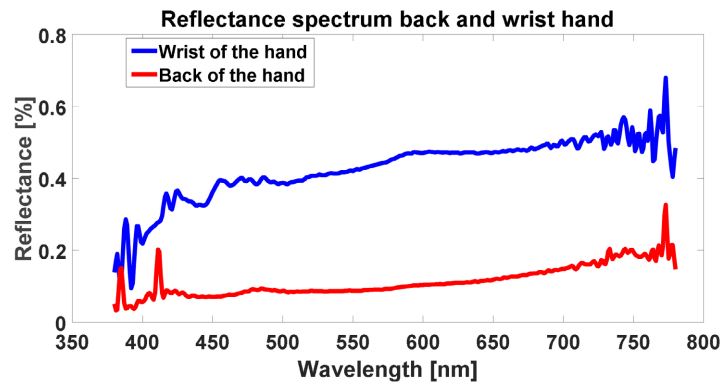


Figure 5. Comparison between the reflectance spectrum of the wrist and the back of the hand.



Figure 6. Standardized photos of the diseased foot.

Note that the wrist reflectance spectrum is ahead of the wrist reflectance spectrum with a significant peak at 382 nm for reflectance of 0.19%. This means that the wrist of the hand is more sensitive than the back of the hand. At 773 nm, the two are in phase, the reflectance is 0.68%.

4. Measurement of the Diffuse Reflectance of a Sick Skin and Analysis of the Measurements

This study was conducted on skin. For this purpose, a panel of thirty volunteers with reddened skin surfaces was selected. The measurements were performed on skin surfaces without any agent or product application. We acquired diffuse reflectance spectra with our instrument (**Figure 6**). In addition, two images of the foot were acquired with a standardized system: from view, left view and right view.

Measurement Results

The analysis of the optical properties obtained with the DRS instrument allows

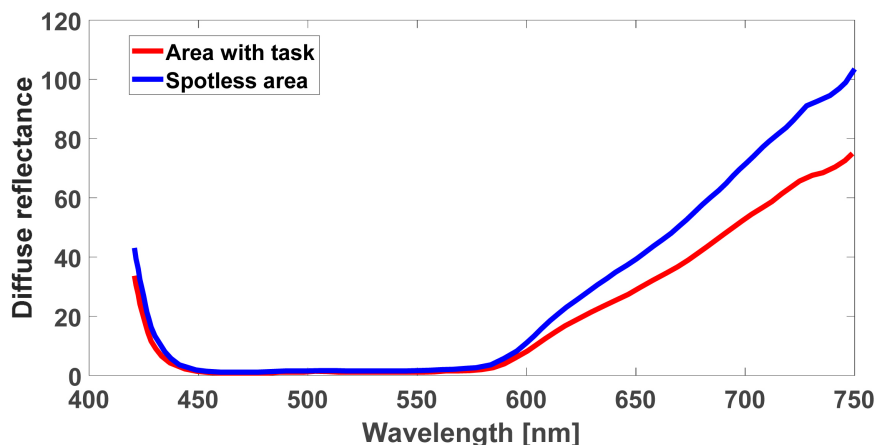


Figure 7. Comparison between a reflectance parameter of the task area and healthy areas.

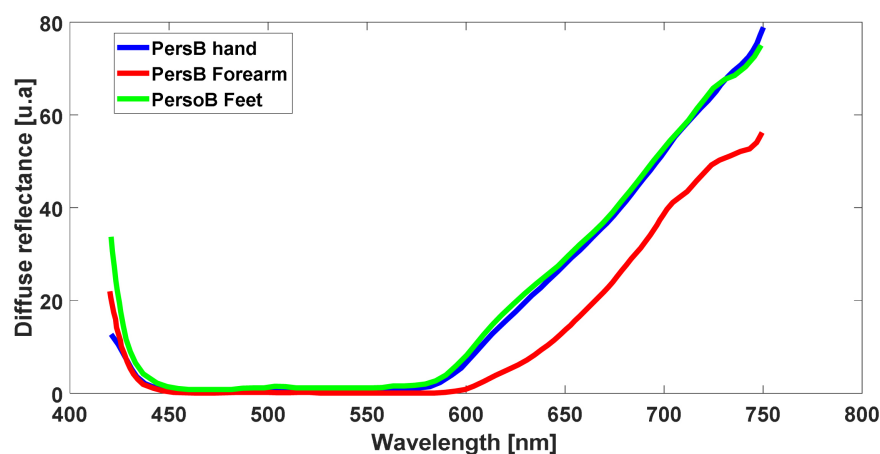


Figure 8. Diffuse reflectance spectrum of person B.

us to observe a coincidence of the spectra of reflectance of the zone with spot and the zone without a spot in the region of the spectra of reflectance from 450 nm to 550 nm. This spectral region seems to correspond to the normal zone. From 550 nm, the start of an infection, the reflectance spectrum of the area with a spot increase rapidly (**Figure 7**). In addition, we carried out measurements in different parts of the arm. The DRS highlights a phenomenon of the evolution of the spectra represented in **Figure 8**.

5. Conclusion

The results presented here demonstrate that diffuse reflectance spectroscopy is a potentially valuable tool for improving the diagnosis of healthy skin and skin lesions or diseases. This method is non-traumatic and avoids biopsy and is also inexpensive and quick. It can only be applied to a shallow depth under the dermis or the mucous membranes, but its range of action can also extend to a large number of skin pathologies such as skin cancers for example. Based on a simple model of healthy skin and skin close to lesions and for skin with different characteristics and levels of melanin, we showed that diffuse reflectance spectroscopy

py could make it possible to obtain different signatures depending on the sites, test and over a wide spectral range. Moreover, a numerical simulation showed that finer discrimination was possible. These preliminary results obtained made it possible to establish the feasibility of the method as well as the establishment of a clinical protocol.

Additional studies are in progress on inert infected tissues at different stages of the disease in order to increase the reliability of the method whatever the skin type and the area of infection.

Acknowledgements

We would like to thank the Service Cooperation and Cultural Action (SCAC) for the funding of this project.

Conflicts of Interest

The authors declare no conflicts of interest regarding the publication of this paper.

References

- [1] Koenig, A., Roig, B., Le Digabel, J., Josse, G. and Dinten, J.M. (2015) Accessing Deep Optical Properties of Skin Using Diffuse Reflectance Spectroscopy. *Clinical and Biomedical Spectroscopy and Imaging IV*, **9537**, 95370E. <https://doi.org/10.1364/ECBO.2015.95370E>
- [2] Kondepati, V.R., Heise, H.M. and Backhaus, J. (2008) Recent Applications of Near-Infrared Spectroscopy in Cancer Diagnosis and Therapy. *Analytical and Bioanalytical Chemistry*, **390**, 125-139. <https://doi.org/10.1007/s00216-007-1651-y>
- [3] McIntosh, L.M., Summers, R., Jackson, M., Mantsch, H.H., Mansfield, J.R., Howlett, M. and Toole, J.W. (2001) Towards Non-Invasive Screening of Skin Lesions by Near-Infrared Spectroscopy. *Journal of Investigative Dermatology*, **116**, 175-181. <https://doi.org/10.1046/j.1523-1747.2001.00212.x>
- [4] Cugmas, B., Bürmen, M., Bregar, M., Pernuš, F. and Likar, B. (2013) Pressure-Induced Near Infrared Spectra Response as a Valuable Source of Information for Soft Tissue Classification. *Journal of Biomedical Optics*, **18**, Article ID: 047002. <https://doi.org/10.1117/1.JBO.18.4.047002>
- [5] Cross, K.M., Leonardi, L., Payette, J.R., Gomez, M., Levasseur, M.A., Schattka, B.J. and Fish, J.S. (2007) Clinical Utilization of Near-Infrared Spectroscopy Devices for Burn Depth Assessment. *Wound Repair and Regeneration*, **15**, 332-340. <https://doi.org/10.1111/j.1524-475X.2007.00235.x>
- [6] Pellicer, A. and del Carmen Bravo, M. (2011) Near-Infrared Spectroscopy: A Methodology-Focused Review. *Seminars in Fetal and Neonatal Medicine*, **16**, 42-49. <https://doi.org/10.1016/j.siny.2010.05.003>
- [7] Scheeren, T.W.L., Schober, P. and Schwarte, L.A. (2012) Monitoring Tissue Oxygenation by Near Infrared Spectroscopy (NIRS): Background and Current Applications. *Journal of Clinical Monitoring and Computing*, **26**, 279-287. <https://doi.org/10.1007/s10877-012-9348-y>
- [8] Xu, K.X., Qiu, Q.J., Jiang, J.Y. and Yang, X.Y. (2005) Non-Invasive Glucose Sensing with Near-Infrared Spectroscopy Enhanced by Optical Measurement Conditions Reproduction Technique. *Optics and Lasers in Engineering*, **43**, 1096-1106.

- <https://doi.org/10.1016/j.optlaseng.2004.06.018>
- [9] Kollias, N. and Stamatias, G.N. (2002) Optical Non-Invasive Approaches to Diagnosis of Skin Diseases. *Journal of Investigative Dermatology Symposium Proceedings*, **7**, 64-75. <https://doi.org/10.1046/j.1523-1747.2002.19635.x>
- [10] Kim, A. and Wilson, B.C. (2010) Measurement of *Ex Vivo* and *In Vivo* Tissue Optical Properties: Methods and Theories. In: Welch, A. and van Gemert, M., Eds., *Optical-Thermal Response of Laser-Irradiated Tissue*, Springer, Dordrecht, 267-319. https://doi.org/10.1007/978-90-481-8831-4_8
- [11] Lafrance, D., Lands, L.C. and Burns, D.H. (2004) *In Vivo* Lactate Measurement in Human Tissue by Near-Infrared Diffuse Reflectance Spectroscopy. *Vibrational Spectroscopy*, **36**, 195-202. <https://doi.org/10.1016/j.vibspec.2004.01.020>
- [12] Yu, L.Y. and Xiang, B.R. (2008) Quantitative Determination of Acyclovir in Plasma by Near Infrared Spectroscopy. *Microchemical Journal*, **90**, 63-66. <https://doi.org/10.1016/j.microc.2008.03.006>
- [13] Bevilacqua, F., Pigué, D., Marquet, P., Gross, J.D., Tromberg, B.J. and Deppeurging, C. (1999) *In Vivo* Local Determination of Tissue Optical Properties: Applications to Human Brain. *Applied Optics*, **38**, 4939-4950. <https://doi.org/10.1364/AO.38.004939>
- [14] Zonios, G., Perelman, L.T., Backman, V., Manoharan, R., Fitzmaurice, M., van Dam, J. and Feld, M.S. (1999) Diffuse Reflectance Spectroscopy of Human Adenomatous Colon Polyps *in Vivo*. *Applied Optics*, **38**, 6628-6637. <https://doi.org/10.1364/AO.38.006628>
- [15] Bashkatov, A.N., Genina, E.A., Kochubey, V.I. and Tuchin, V.V. (2005) Optical Properties of Human Skin, Subcutaneous and Mucous Tissues in the Wavelength Range from 400 to 2000 nm. *Journal of Physics D: Applied Physics*, **38**, Article 2543. <https://doi.org/10.1088/0022-3727/38/15/004>
- [16] Gendrin, C., Roggo, Y. and Collet, C. (2008) Pharmaceutical Applications of Vibrational Chemical Imaging and Chemometrics: A Review. *Journal of Pharmaceutical and Biomedical Analysis*, **48**, 533-553. <https://doi.org/10.1016/j.jpba.2008.08.014>
- [17] Yable, D.K. Canale, L. Haba, T.C. Kyrginas, D. Dupuis, P. and Zisis, G. (2021) A Novel Optical Design by Ultraviolet Visible-Near Infrared Absorption Spectroscopy with Dual Elliptical Reflectors for the Detection of Mycobacterium Ulcerans. 2021 *IEEE International Conference on Environment and Electrical Engineering and 2021 IEEE Industrial and Commercial Power Systems Europe (EEEIC/I&CPS Europe)*, Bari, 7-10 September 2021, 1-6. <https://doi.org/10.1109/EEEIC/ICPSEurope51590.2021.9584792>